External Characteristics of Unsteady Spray Atomization from a Nasal Spray Device

MAN CHIU FUNG,[1] KIAO INTHAVONG,[1,2] WILLIAM YANG,[3] PETROS LAPPAS,[1,2] JIYUAN TU[1,2]

[1]School of Aerospace, Mechanical and Manufacturing Engineering, RMIT University, Bundoora, Victoria 3083, Australia

[2]Platform Technologies Research Institute, RMIT University, Bundoora, Victoria 3083, Australia

[3]CSIRO Process Science and Engineering, Clayton South, Victoria, Australia

Received 1 October 2012; revised 13 November 2012; accepted 21 December 2012

Published online 9 January 2013 in Wiley Online Library (wileyonlinelibrary.com). DOI 10.1002/jps.23449

ABSTRACT: The nasal route presents an enormous opportunity to exploit the highly vascularized respiratory airway for systemic drug delivery to provide more rapid onset of therapy and reduced drug degradation compared with conventional oral routes. The dynamics of atomization at low injection pressure is less known as typical spray atomization studies have focused on industrial applications such as fuel injection that are performed at much higher pressure. An experimental test station was designed in house and an alternative method to characterize the external spray is presented. This involved the use of high-speed camera to capture the temporal development of the spray as it is atomized through actuation of the spray device. An image-processing technique based on edge detection was developed to automate processing through the large number of images captured. The results showed that there are three main phases of spray development (prestable, stable, and poststable) that can be correlated by examining the spray width. A comparison with a human nasal cavity is made to put into perspective the dimensions and geometry that the spray atomization produces. This study aimed to extend the current existing set of data to contribute toward a better understanding in nasal spray drug delivery. © 2013 Wiley Periodicals, Inc. and the American Pharmacists Association J Pharm Sci 102:1024–1035, 2013

Keywords: nasal drug delivery; targeted drug delivery; computer aided drug design; aerosol; high-speed camera; imaging methods; spray atomization

INTRODUCTION

The efficacy of nasal spray drug delivery is mainly dependent on parameters such as drug formulation,[1,2] spray atomization,[3,4] spray device,[5] and patient handling.[6,7] Experimental and numerical studies in the literature for improved nasal drug delivery can be categorized into two fields: (1) external and internal characteristics of spray atomization from the nasal spray device,[8,9] and (2) transport and deposition of spray droplets in the nasal cavity.[10]

Experiments of the droplet deposition in the nasal cavity from nasal spray devices have been performed by Cheng et al.[11] wherein magnetic resonance imaging scans of a human nasal cavity was used to create a replica airway model. The results showed that the narrow airway passage in the nasal cavity limits the development of the spray plume and the dispersion of spray droplets inside nasal cavity. Furthermore, the study recognized the impact of inhalation flow rate and aerosol size on deposition efficiency. Suman et al.[12] allowed volunteers to operate nasal sprays that contained ^{99m}technetium-labeled spray droplets. The regional deposition of spray droplets in nasal cavity was captured by gamma scintigraphy and the results concluded that the droplet size emitted from nasal spray bottle has a significant effect on drug delivery. Therefore, by controlling the droplet size distribution (DSD), targeted deposition patterns may be attained.

Dayal et al.[1] showed that the use of bioadhesive polymers (used to increase residence time and drug absorption) increases viscosity and also has an impact on the DSD. Furthermore, different drug formulations for therapeutic effects will also exhibit different fluid properties. Therefore, alternative means

Correspondence to: Jiyuan Tu (Telephone: +61-3-9925-6191; Fax: +61-3-9925-6108; E-mail: jiyuan.tu@rmit.edu.au)

Journal of Pharmaceutical Sciences, Vol. 102, 1024–1035 (2013)

to control the DSD should be investigated to provide flexibility in drug developments. A study by Kippax et al.[6] using laser Doppler anemometry showed that different DSDs are produced for different actuation parameters that included actuation force and speed. The variation in actuation parameters is most evident among different age groups (e.g., child vs. adult), which has also been confirmed by Doughty et al.[13] This study presents actuation profiles and its variation against actuation force, hold force, and release force. The compression velocity, hold time, and release velocity of nasal spray nozzle and the average spray weight produced by adult and child users were correlated with the use of a linear displacement transducer. It should be noted that no actual DSD data were produced. However, the results are significant for correlating machine-actuated stations to real-life user actuations to provide *in vitro* bioequivalence testing of nasal aerosols as set out by the US Food and Drug Administration (FDA) draft guidance document.[14]

Guo and Doub[2] and then later Guo et al.[7] and Liu et al.[15] studied the influence of actuation parameters by an automated system, including shot weight, stroke length, and stroke velocity on the spray pattern and DSD. The actuation parameters were measured by electronic automated actuation system; spray external characteristics by high-speed camera and DSD were analyzed by laser diffraction system. Stroke length and actuation velocity are found to have significant impact on DSD and spray pattern, whereas the shot weight is the least sensitive characteristics to the variation of actuation parameters. Velocity profiling of nasal spray pumps were also performed by Williams et al.[16]

By studying the atomization process, DSD as well as spray characteristics such as spray velocity, angle, and penetration can be found. Recently, Inthavong et al.[17,18] applied particle image velocimetry and particle/droplet image analysis (PDIA) to study the continuous spray from nasal spray device. The study highlighted the importance of understanding local characteristics of spray development within its surrounding because the limitation of the narrow cross section of the nasal cavity does not allow the full development of a spray plume. The experimental studies reviewed provide important data for researchers using computational fluid dynamics (CFD) to simulate the transport and deposition of inhaled drug particles.[19–23] Such CFD studies have evaluated different spray delivery parameters (spray cone angle, droplet velocity, particle size, insertion angle, and particle release location) on deposition efficiency.[24,25]

The objective of this study is to extend the current set of data obtained in the author's earlier work[3] on the external characteristics of a nasal spray during a steady stream of flow. The work presented in this paper extends the previous study by investigating the atomization and spray development in a time-dependent mode. Furthermore, the difference is not only temporal, but also spatial because the spray is now ejected vertically upward in this study, which is more realistic in terms of a typical nasal spray operation performed by patients. An automated actuation system under different loads is also applied to simulate different strengths in actuation performance. Current methods for nasal spray characterization have used the laser diffraction technique to characterize the beginning, middle, and end of the plume, and such measurements should be made at three distances from the delivery orifice (FDA Guidance Draft). However, this study reports the use of high-speed photography, and image-processing algorithms that have been developed in house are used to determine the external spray characteristics including the three phases of plume development.

METHODS

The experimental setup consists of an automated actuation system consisting of an actuation station that contains the spray device, a programmable logic control (PLC) unit, water supply, and a visualization

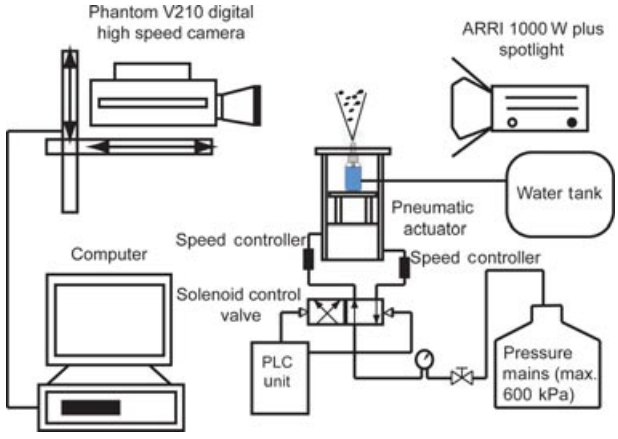

Figure 1. A schematic of the experimental setup showing the automated actuation system and the visualization system.

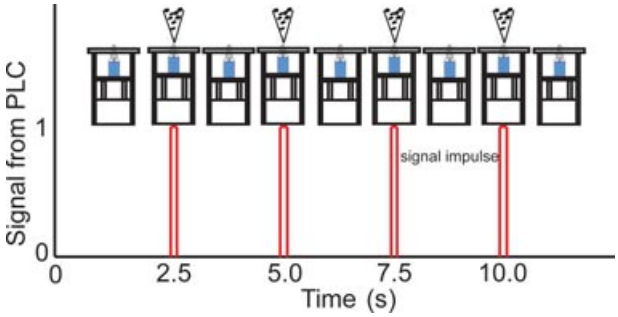

Figure 2. Signal profile sent from the PLC unit to activate/deactivate the control valves.

system consisting of high-speed filming with shadowgraphy.

Automated Mechanical Actuation System

A schematic of the experimental setup is shown in Figure 1, which has an automated actuation system designed and built in house. The pneumatic actuator (model: SMC-CXSL10-10; ADI, Inc., Hatfield, Pennsylvania) is connected to a two-way solenoid valve, which is controlled by a PLC unit (model: 1760-L12BWB; Allen Bradley, Lumberton, New Jersey). The spray bottle is fixed at its base onto the actuator, to avoid the undesired lateral motion during actuation. During actuation, the spray bottle moves up and down with the platform on which it is placed, whereas the spray nozzle remains at one position. This allows the visualization system to capture images with a fixed reference point. The strength of actuation force is controlled by the backpressure supplied by a connection to a pressure line.

Speed controllers (model: SMC-AS2002F-06; Allied Electronics, Inc., Fort Worth, Texas) are installed on the two plastic tubes connecting the actuator and solenoid to control the flow rate of the compressed air. Because of pressure losses and the effect of the speed controllers, the resultant peak pressure that is imparted onto the actuator was monitored and found to be 2.05, 2.45, and 2.65 bar. Hence, the actuation speed related to pressing down (extension of actuators) and releasing (contraction of actuators) of a nasal spray device can be managed and matched to realistic human use. The PLC unit switches the solenoid on and off by sending simple on–off logic signals. The actuation profile is shown in Figure 2. First, the nasal spray bottle is held at its rest position for 2.5 s, then a signal pulse (which is synchronized to a computer and camera) is sent to extend the actuator, which forces the spray bottle upward. The signal pulse duration is 80, 120, and 180 ms for three different actuation cases, which is dependent on the actuation speed. The actuator then retracts back to its rest position after completing a full actuation. This cycle is then repeated as needed. The time between each actuation was set to 2.5 s by using a PDIA to determine the sufficient settling time for residual droplets in the air to disappear before the next cycle. This is checked by examining photo pairs captured by PDIA, with a time difference of 10 μs, to ensure that no residual droplets are found in the image.

The spray bottle used is a commercially available nasal spray device (Beconase Hayfever device kindly provided by GlaxoSmithKline) capable of delivering 180 sprays per bottle with 50 μg/metered spray of formulation as described on the product label. To ensure a consistent pressure within the spray bottle during the experiment, a large water tank (20 L) filled with distilled water was attached to the nasal spray bottle that supplies water and enables a consistent water level in the nasal spray bottle.

A single bottle is used to focus on the alternative method for spray actuation by using a customized experimental setup and to explore the different stages

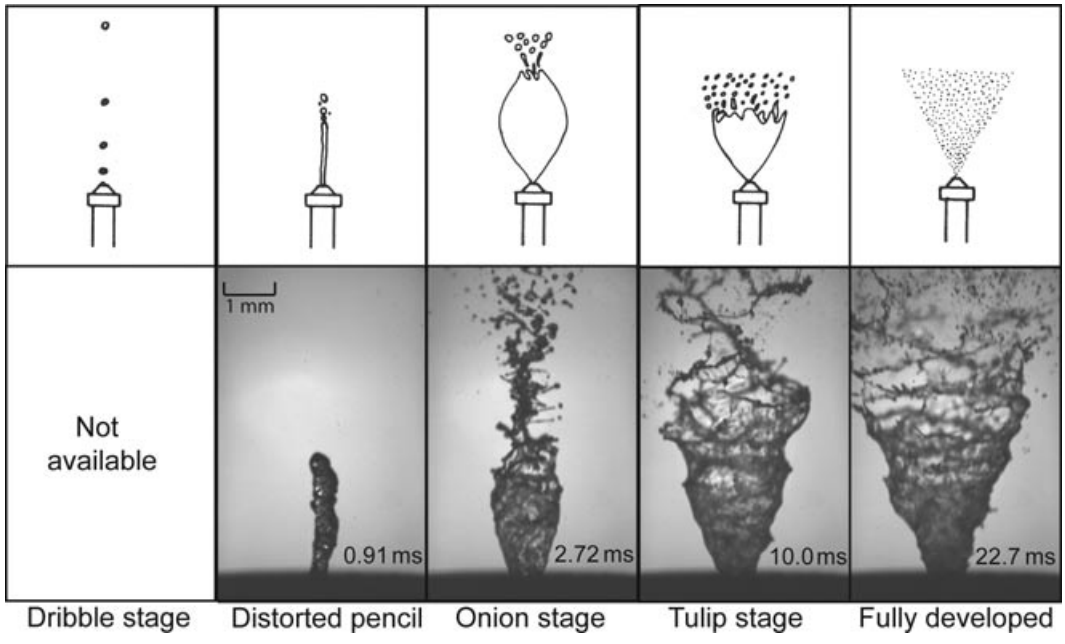

Figure 3. Comparison of spray development stages of nasal spray device under 2.65bar compression pressure with schematic from Lefebvre[28]: distorted pencil, onion stage, tulip stage, and fully developed. Dribble stage is only available at higher backpressure.

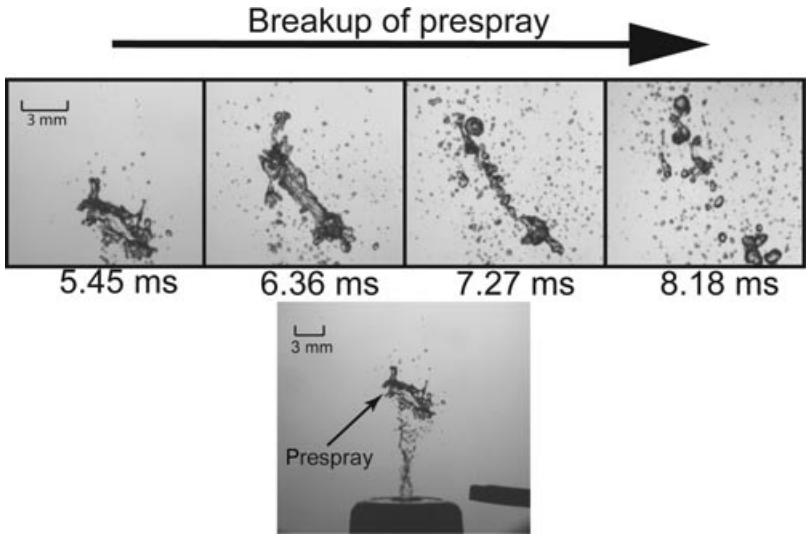

Figure 4. Formation of prespray because of the insufficient compression pressure at initial stage. Prespray will further breakup into large water blob by aerodynamic force when travel further downstream. The time is counted from the moment when spray nozzle was being pressed.

that occur in drug delivery. It should be expected that although plume profiles will differ for different devices, the characteristics of atomization stages are similar. This is also apparent for different drug formulations. The different viscosities and the surface tension properties will alter the atomization process. Therefore, the results herein are standardized against water as its formulation. The influence of different formulations on atomization and droplet formation has been reported by Dayal et al.[1]

Visualization System

The actuation station was placed between a high-speed camera and a powerful ARRI 1000 W tungsten spotlight (ARRI Group, Munich, Germany) to produce a shadowgraph images. An additional spotlight was used to allow shorter exposure times. Spray images were captured by a Phantom V210 digital high-speed camera with 1280 × 800 CMOS sensor (ViSiON Research, Wayne, New Jersey). The frame rate and exposure time were 2200/s (i.e., 0.45 ms) and 6 μs, respectively. Photo images of the spray bottle motion (during pressing, holding, and releasing) and the development of spray plume (expanding of spray cone, fully developed spray cone, and collapsing spray cone) were captured. Up to 10 sets of images were captured for each different actuation pressure (2.05, 2.45, and 2.65 bar); however, some sets were discarded when obvious spurious spray variations occurred because of errors caused by handling, timing, and system setup problems. To ensure consistency and repeatability, the high-speed filming is performed before and after 200 actuations to compare the external spray characteristics. The displacement of the spray bottle and the pneumatic actuator was filmed separately from the actual spray atomization. The time history of nozzle displacement and velocity was then able to compare with the development of spray plume during image acquisition.

The captured images (approximately 3000 images per actuation) are analyzed using in-house developed computational image-processing programs created within MATLAB (MathWorks, Natick, Massachusetts) to obtain the spray width. The photographs were converted to binary image, and the Canny edge detection[26] algorithm was used to calculate the boundary of the spray cone. The boundary was determined by finding the greatest gradient of change of the intensity of pixels. The boundary has a non-zero pixel value, and the background has a pixel value of zero (black). By converting the number of pixels with value of zero between the two edges of spray cone, spray width can be obtained for analysis. This same process has also been reported by Inthavong et al.[4]

RESULTS AND DISCUSSION

Spray Atomization

A previous study by the authors[4] has determined that the atomizer used in the nasal spray device is of a pressure swirl type. The theories presented by Lin and Reitz,[27] and Lefebvre[28] describe the spray development through several stages as the liquid injection pressure is increased from its initial resting state. Figure 3 shows these stages, which are the dribble, distorted pencil, onion, tulip, and fully developed stages. The recorded time shown is the time from when the liquid is first ejected from the nozzle.

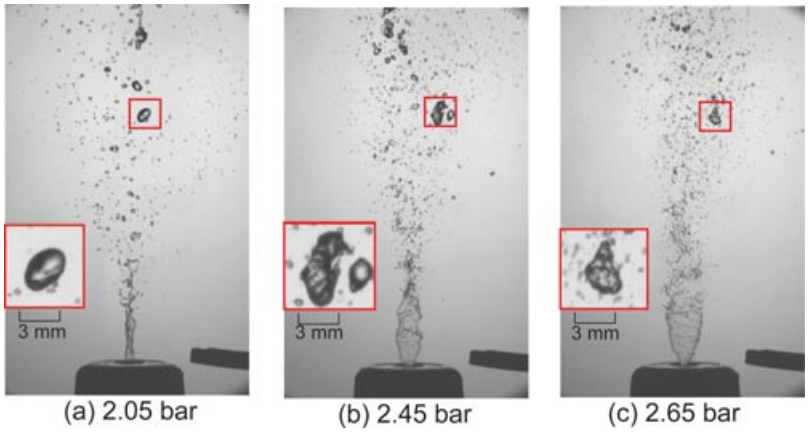

Figure 5. The maximum width of the last water blob formed by prespray under different injection pressure.

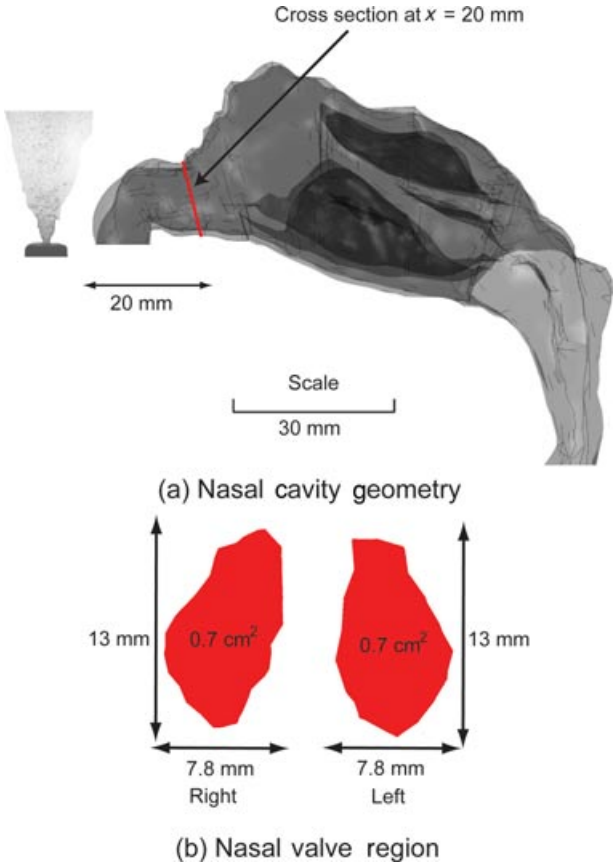

Figure 6. (a) A scaled schematic showing the geometry of a fully developed spray in relation to a nasal cavity geometry. (b) A cross-sectioned view of a slice in the nasal valve region (which has smallest cross-sectional area in nasal cavity[29]) taken at 20 mm from anterior tip of nose.

There is some lag between it and the time of first bottle movement due to the applied force having to overcome the internal spring. During the spray development from atomization, it was found that each of the stages occurs except for the dribble stage. This stage only occurs when the pressure is low enough to produce small dribbling droplets. It can be seen that the distorted pencil is narrow and develops up to 2.6 mm before breaking up to form an onion stage shape. The development length of the distorted pencil is similar to the dimensions of a typical adult nostril region. This means that the orientation of the spray device should be inserted into the nose angled in line with the main nasal passage. This would provide sufficient clearance from the nostril region and allow the spray to develop beyond the distorted pencil stage, and full atomization to occur within the main nasal passage.

A closer inspection of all captured data showed that large droplets were formed consistently before the main breakup of the liquid occurred (Fig. 4). To ensure that this prespray breakup was not a consequence of residual water from the previous spray actuation, an absorbent material was used to clear away any liquid that was present in the nozzle recess of the spray before the next spray actuation was performed each time. The large droplets during prespray were observed in every measurement taken. It is inferred that this is caused by the lower injection pressure present early in the atomization process causing the bulk liquid to exit without breaking up and instead liquid ligaments are formed, which break up further into large water droplets, because of the aerodynamic instability. A sample demonstrating the resultant large droplet occurring from the prespray breakup is shown in Figure 5 for 2.05, 2.45, and 2.65 bar cases. This is highlighted as it contributes toward early droplet deposition in the nasal cavity. Morphometric data of the nasal cavity presented in Wen et al.[29] show that the minimum cross-sectional area in each nasal chamber is approximately 0.7 cm^2, which occurs at around 20 mm from anterior tip of

 DOI 10.1002/jps

nose for a young and healthy Asian male (Fig. 6). Taking a cross-sectional slice, the geometry in two dimensions shows that the width is 7.8 mm and the height is 13 mm.

Previous results but under a steady 5 bar pressure, showed that the atomization produced a volume equivalent to averaged diameter ($D_{30,ave}$ ~60 μm) from the same nasal spray device{Fung, 2012 #25}. From numerical results of deposition by Inthavong et al.,[18] spray droplets with 20 μm under normal breathing condition hit the nasal vestibule immediately. The likelihood of droplet deposition is highly dependent on the droplet inertia, which is usually described through either the inertial parameter, $IP = d^2_{as}\,Q$ (where d^2_{as} is the aerodynamic diameter, and Q is the inhalation rate), or the droplet Stokes number, $\rho d^2_{as} U/18\mu D$, where ρis the droplet density, U is the flow velocity, D is the characteristic length, and μ is the fluid viscosity. This implies that the apart from the external spray characteristics, deposition is highly sensitive to the droplet size, but it can also influenced by inhalation rate and the nostril geometry.

Characterization of Spray Phases

The use of laser diffraction to characterize the beginning, middle, and end of the plume is a method for nasal spray characterization, with measurements taken at three distances from the orifice (FDA Guidance Draft[14]). Kippax et al.[6] and Suman et al.[12] used laser diffraction to find the DSD profile during spray atomization, wherein a decreasing DSD occurred at the beginning, a stable region was found in the middle phases, and finally an increasing DSD at the end. This profile is typical of spray atomization wherein the low pressure encountered at the beginning and end of spray development produces a decreasing and increasing DSD, respectively, forming a U-shaped profile. Therefore, there is a stable phase wherein the droplet size becomes small and relatively constant during the atomization process, and can be defined as the "stable phase" or the middle of the spray plume development as suggested by the FDA Guidance Draft. From the numerical simulation by Snyder et al.,[30] it was shown that the spray droplet size is inversely proportional to the spray cone angle. Hence, we can conclude that the spray droplet size will be smallest

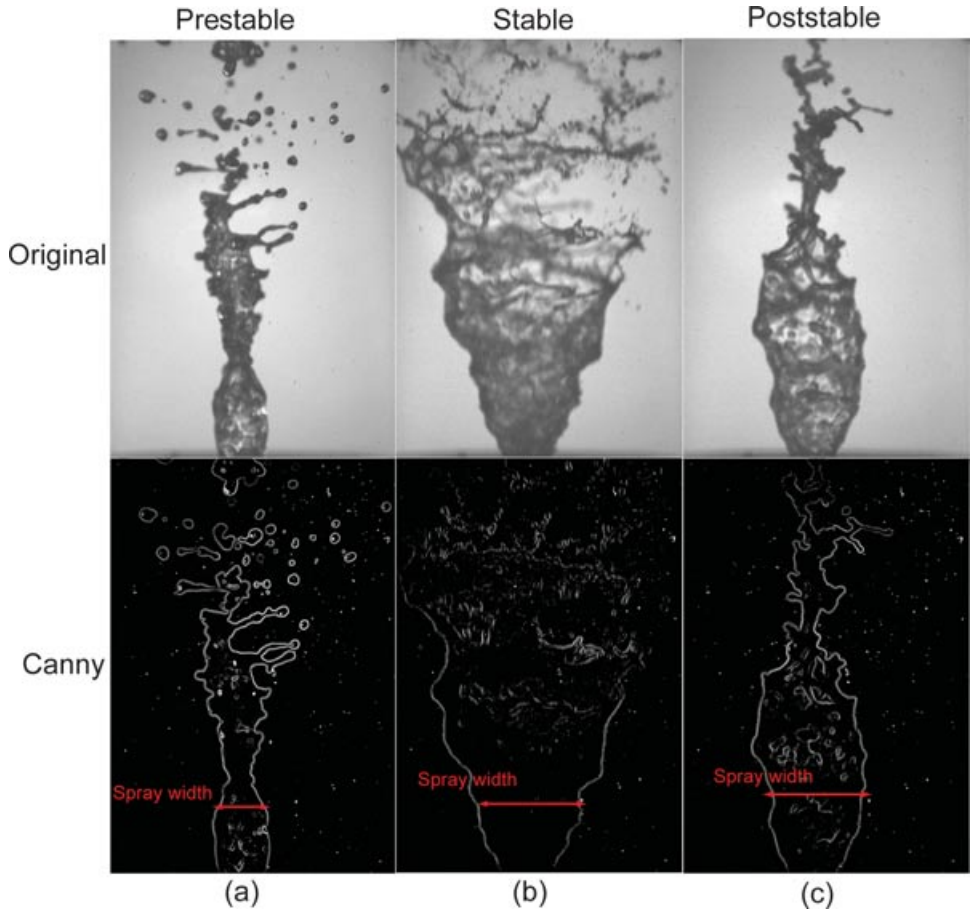

Figure 7. The spray photos at prestable, stable, and poststable phases were processed using the Canny edge detection. The edge of spray cone can be traced by white outlines. The spray width at 1.5 mm downstream was defined as the distance between the white boundaries.

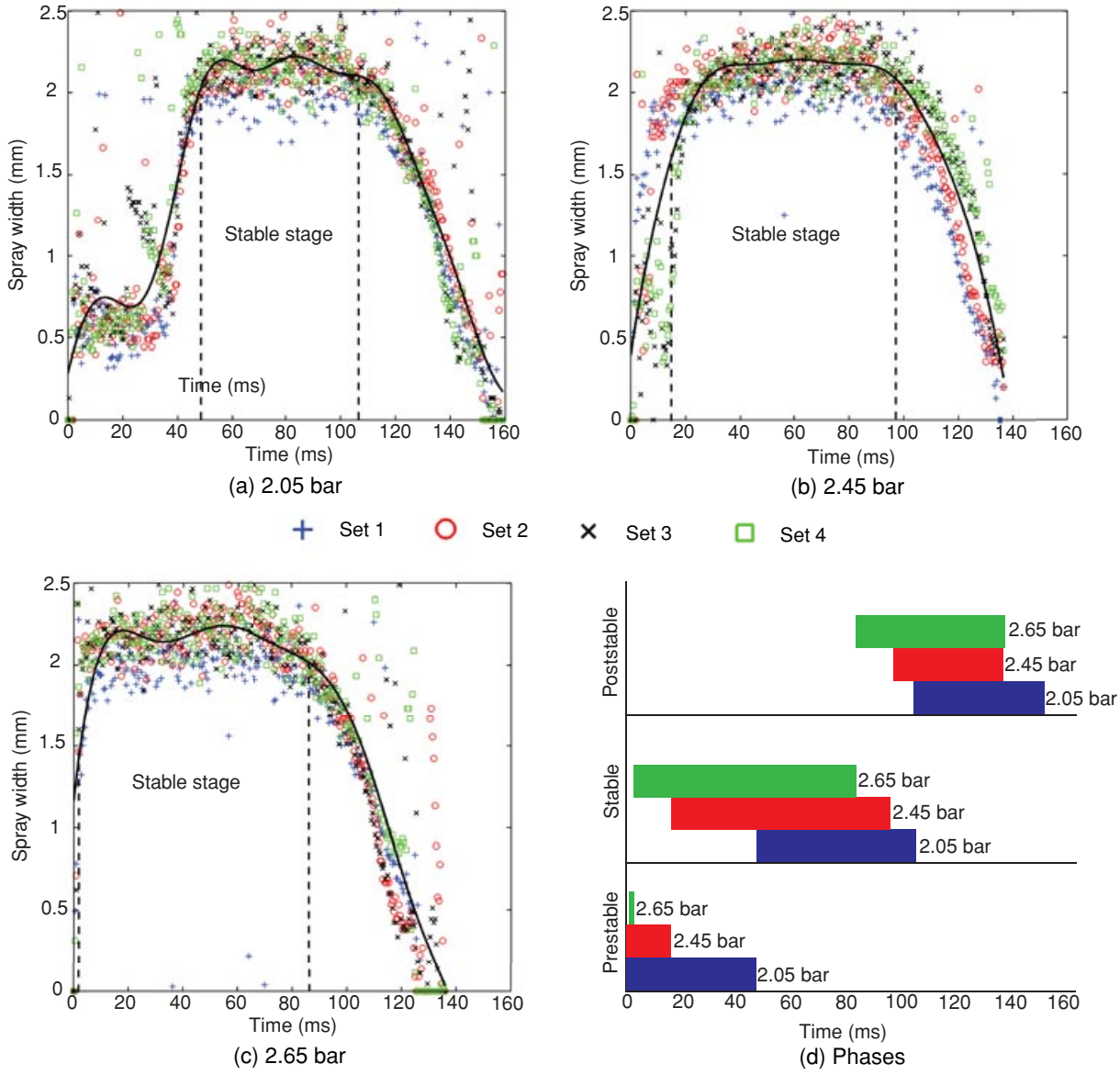

Figure 8. The variation of spray width at 1.5 mm downstream from injection point under injection pressures of (a) 2.05 bar, (b) 2.45 bar, and (c) 2.65 bar. (d) Phases of spray periods relative for each injection pressure.

when the spray cone width reaches its maximum and thus reaches the stable phase.

The spray width in each captured image is analyzed using image-processing codes developed in MATLAB (MathWorks). The spray cone width is measured by finding each pair of white pixels and this is obtained at three downstream distances (1.5, 3.0, and 4.5 mm) from the nozzle. Although all sets of data for the different downstream distances provided a consistent trend among the results, the distance at 1.5 mm was used for further analysis as it provided the best set of data to reveal the variation of spray cone development during atomization (Fig. 7).

The spray width plotted against spray time for each pressure case is given in Figure 8. The results show a clustering of data points into three distinct regions with individual outliers surrounding the each cluster. A curve fit using sum of four sine functions is applied to give a clearer visualization of the trending data. Although the spray cone development is a continuous process, the clustering of data points show that a quasi-discontinuous step profile is apparent. The different phases are defined by analyzing the variation of standard deviation of the data points for a given clustering range of data and shown in Figure 8 with dashed lines.

 DOI 10.1002/jps

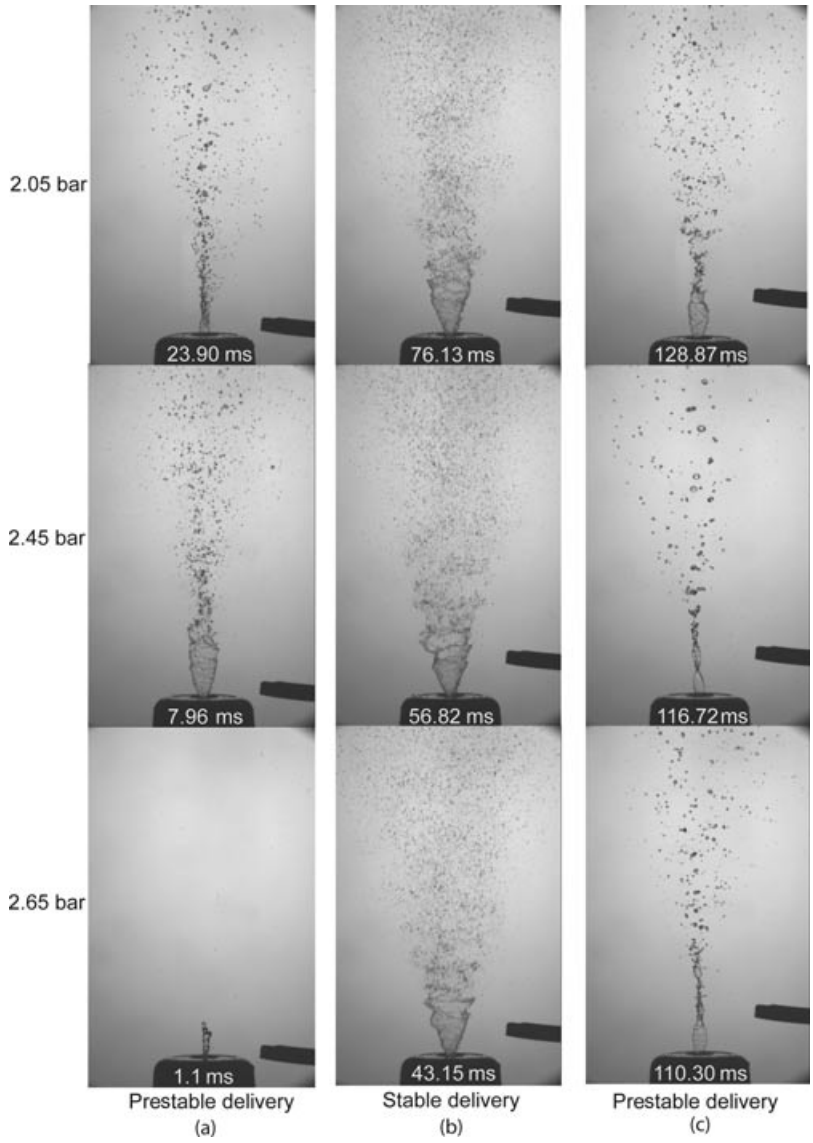

Figure 9. The visualization of spray cone at the middle of (a) prestable, (b) stable, and (c) poststable delivery phases under 2.05, 2.45, and 2.65 bar backpressure. The time showing is the middle of each phase and is counted from the start of the compression of nasal spray nozzle.

The exact time for each phase is given in Figure 9, wherein each phase for each pressure case is compared against each other. It can be seen that at high pressure, there is a rapid progression in reaching the stable phase and thus a rapid progression towards a smaller DSD. The stable and poststable phases for all injection pressures are relatively similar in duration. For a pressure of 2.05 bar, the prestable phase is the longest and this implies that larger droplets are produced. From these results and earlier numerical studies by the authors,[19,31] an inference on the efficacy of sprayed drug particles based on fluid–droplet dynamics can be made. The atomized droplets exist in the micron-sized range, which deposit in the nasal cavity by inertial impaction. Neglecting droplet breakup, the fluid–droplet dynamics primarily relies on the particle relaxation time $\frac{\rho d_p^2}{(18\mu)}$ (which is essentially a measure of the droplet inertia because of its size) and the moving fluid velocity that transports the droplet. Although the 2.65 bar case produces a highly rapid acceleration of droplets during the initial atomization, it produces a greater number of smaller droplets in the stable phase, and it is the droplet size that is most sensitive to droplet inertia (i.e., $d^2{}_p$ as given in the particle relaxation correlation). This means that a higher spray pressure producing finer droplets will more likely produce better conditions for nasal drug delivery (Fig. 10). Figure 10 also provides insight into the typical DSD produced at the different phases of spray development caused by the different actuation

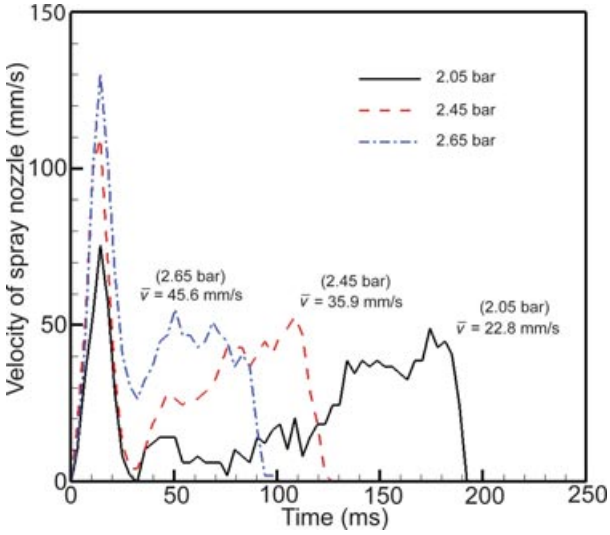

Figure 10. Comparison of the history of spray nozzle velocity under different backpressures. The average velocity of spray nozzle for the prestable, stable, and poststable delivery phases is also indicated. According to the work by Doughty et al.,[32] the average velocity of the compression of spray nozzle is 23.54 and 41.87 mm/s for pediatric and adult, respectively.

pressure settings and its relationship with a subject's inhalation profile. For example, if a droplet has too low inertia, then these droplets are likely to pass through the nasal cavity and therefore it may be instructive for a subject exhibiting high actuation strength to inhale more rapidly to increase the small droplets that are produced rapidly.

For visualization purposes, the spray image taken at the midpoint of each phase of spray development is shown in Figure 10. The images for the stable and poststable phases show similar external characteristics, whereas one main difference is found for the high-pressure (2.65 bar) case wherein the prestable phase shows only a small dribble of liquid because of its very rapid atomization. Because images are time dependent, they are useful for qualitative comparisons with CFD simulations of spray atomization development and drug delivery.

Actuation Velocity

Figure 10 shows the velocity profile of the spray nozzle for different spray pressures. It should be noted that the initial start time is set when the nozzle moves, which differs from the earlier figures, wherein the water exits the orifice slightly after the initial actuation. There is a sharp acceleration reaching a peak at around 20 ms as the bottle is compressed. At this stage, the spring inside the atomizer is yet to be compressed and this opposing spring force causes the actuation velocity to decelerate. For the 2.65-bar case, the velocity quickly increases again to a second peak, where the actuation velocity becomes relatively constant before decreasing to rest. This constant section corresponds to the stable phase where the velocities range between 38 and 42 mm/s. This velocity range correlates with the best atomization performance for fine spray droplets for this spray bottle. Theoretically, extending the duration of actuation velocity in this range will increase the generation of finer spray droplets. From Figure 10, it can be seen that the time taken to reach the second peak increases significantly when the pressure is lesser. The average actuation velocities are 22.8, 35.9, and 45.6 mm/s for 2.05, 2.45, and 2.65 bar pressures, respectively. When compared with the research by Doughty et al.,[32] the average velocity of the spray nozzle under 2.05 and 2.65 bar compression pressure by automated actuation corresponds to the hand operation of nasal spray bottle by pediatric and adult patients.

Near-Nozzle Spray Characteristics

As the water is ejected through the pressure swirl atomizer, a swirling liquid sheet is formed at the nozzle exit. This liquid sheet disintegrates into ligaments because of instabilities caused by shearing with the surrounding air. The distance at which this occurs from the spray nozzle is referred to as breakup length (L_{bu}). For the L_{bu}, the oscillating nature of the liquid sheet made it difficult to use the edge detection scheme. applied earlier Instead, visual inspection was performed over 200 images, which proved to be statistically sufficient to get an averaged value for each spray phase and pressure case. Figure 11 summarizes the L_{bu}s and also shows an averaged spray plume by overlaying each individual image onto a single image. The stable phase for all pressure cases has consistent external characteristics (cone shape and dimension). The L_{bu}s for the stable phase ranged from 4.98 to 5.17 mm and the spray half cone angles were about 21°. The standard deviations of the L_{bu} of the three cases were approximately 0.8, and is similar for all pressure cases. The long L_{bu} implies a fine droplet formation, according to the liquid sheet atomization theory by Senecal et al.[33] For the prestable phase, the L_{bu} and half cone angle were more varied. The 2.05 and 2.65-bar cases have short L_{bu}s, but this is skewed by the early injection period where no breakup occurs. As the 2.65-bar case has an extremely short duration (2.2 ms) and unstable in nature, the standard deviation of L_{bu} is large. As stated earlier, the L_{bu} has a close relationship with the droplet size, and an inconsistent L_{bu} implies a diverse spectrum of spray droplet size.

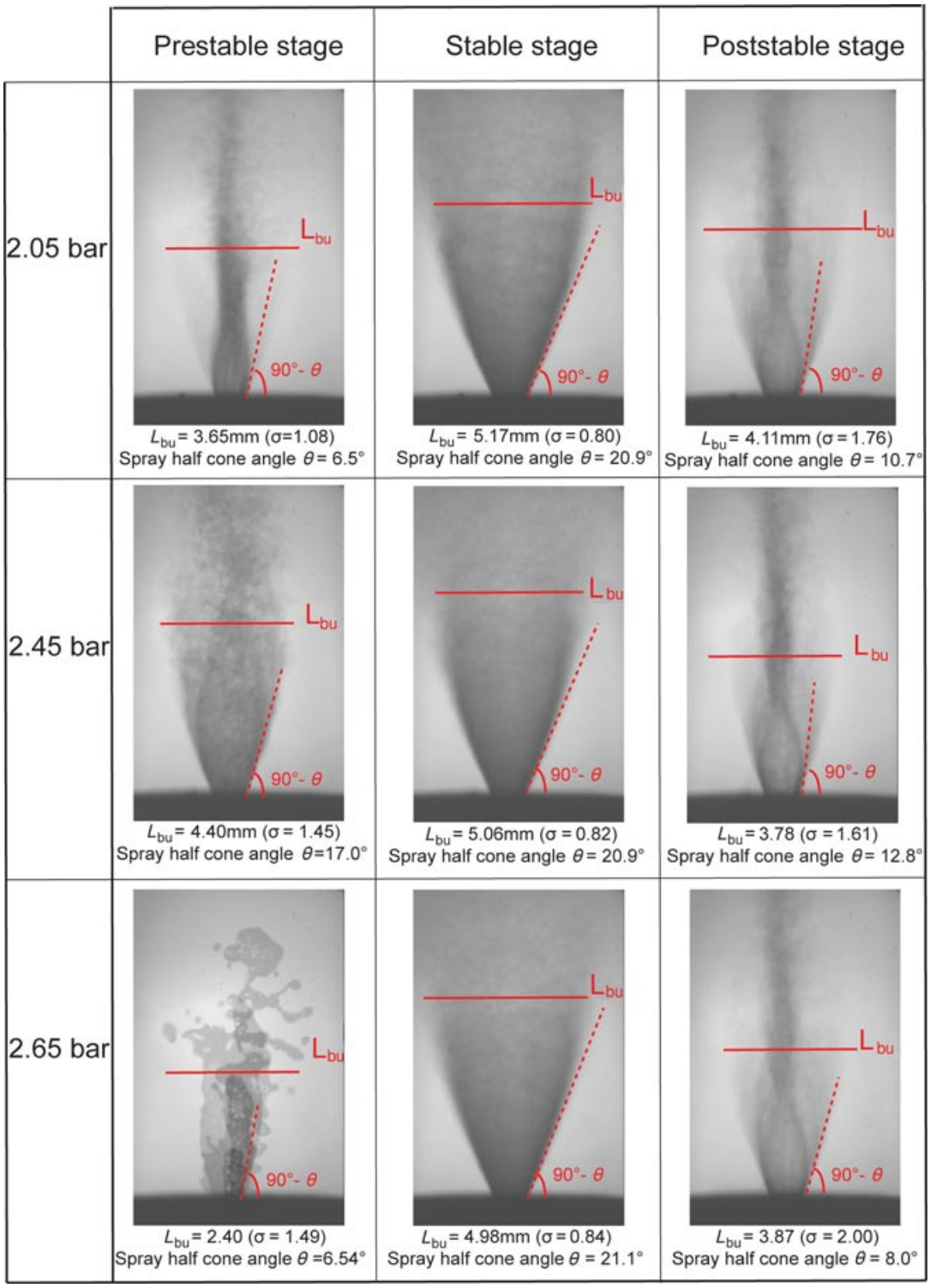

Figure 11. Spray atomization and droplet formation. Breakup length (L_{bu}) is defined as the averaged location of breakup of liquid sheet and formation of ligament in the corresponding spray phase. It is indicated by red line and measured from injection point. Spray half cone angle (θ) is measured to quantify the expansion of spray cone. It is the most significant value of the corresponding spray phase

CONCLUSIONS

This study presented a qualitative study of the external characteristics of an unsteady spray atomization from a nasal spray device. A testing station was built in house for the automated actuation of the spray bottle to replicate hand operation of different subject strengths equivalent to 2.05, 2.45, and 2.65-bar spray pressure. Four distinct developmental stages as described in the literature were captured by the high-speed camera. Interestingly, breakup of large water ligaments and droplets were present during the prespray stage, which has important implications for spray drug delivery given the nasal cavity airway geometry. It is noted that although this phenomena was consistent during all spray measurements, it is left for further investigation as to whether this would be found in other nasal spray devices. Using image-processing techniques, the stable phase of spray atomization was determined based on the spray width as it developed. The duration of each phase was also mapped out for each pressure case, which found that the stable phase persisted the longest. This mapping allows for a better understanding in providing advice to patients on timing, handling, and application of nasal spray actuation. Visualization of the spray in the near nozzle also provided insight into the different external spray structure that included the L_{bu} and spray cone angle which are formed during the different phases. Finally, the velocity profile of the actuation of spray nozzle as it is depressed and its averaged velocity confirmed that the range of actuation strength produced between 2.05 and 2.65 bar is similar to the range from a pediatric to an adult subject. The study investigated the external characteristics of spray development from a single nasal spray device. Further studies on different commercially available nasal sprays and the DSD will further contribute toward a better understanding of spray atomization in medical drug delivery devices.

ACKNOWLEDGMENTS

The authors gratefully acknowledge the financial support provided by the Australian Research Council (project ID: DP120103958).

REFERENCES

1. Dayal P, Shaik MS, Singh M. 2004. Evaluation of different parameters that affect droplet-size distribution from nasal sprays using the Malvern Spraytec. J Pharm Sci 93(7):1725–1742.
2. Guo C, Doub WH. 2006. The influence of actuation parameters on in vitro testing of nasal spray products. J Pharm Sci 95(9):2029–2040.
3. Fung MC, Inthavong K, Yang W, Tu J. 2012. CFD modeling of spray atomization for a nasal spray device. Aerosol Sci Technol 46(11):1219–1226.
4. Inthavong K, Yang W, Fung MC, Tu JY. 2012. External and near-nozzle spray characteristics of a continuous spray atomized from a nasal spray device. Aerosol Sci Technol 46(2):165–177.
5. Doughty DV, Diao L, Hoag SW, Dalby RN. 2010. Use of flexible weighted nasal spray dip tubes to improve product performance. J Aerosol Med Pulm Drug Deliv 23(2):69–75.
6. Kippax PG, Krarup H, Suman JD. 2004. Applications for droplet sizing—Manual versus automated actuation of nasal sprays. Pharm Technol:30–39.
7. Guo C, Stine KJ, Kauffman JF, Doub WH. 2008. Assessment of the influence factors on in vitro testing of nasal sprays using Box–Behnken experimental design. Eur J Pharm Sci 35(5):417–426.
8. Farina D. 2008. Advancing the science of in vitro testing and laboratory data management for nasal sprays. Drug Deliv Technol 4(4):1.
9. Ikeda Y, Yamada N, Kawahara N. 1998. PIV application for spray characteristic measurement. In 9th International Symposium on Application of Laser Techniques to Fluid Mechanics. Lisbon, Portugal.
10. Foo M, Cheng Y, Su W, Donovan M. 2007. The influence of spray properties on intranasal deposition. J Aerosol Med 20[4 (Dec 1)]:495–508.
11. Cheng YS, Holmes TD, Gao J, Guilmette RA, Li S, Surakitbanharn Y, Rowlings C. 2001. Characterization of nasal spray pumps and deposition pattern in a replica of the human nasal airway. J Aerosol Med 14(2):267–280.
12. Suman JD, Laube BL, Lin TC, Brouet G, Dalby R. 2002. Validity of in vitro tests on aqueous spray pumps as surrogates for nasal deposition. Pharm Res 19:1–6.
13. Doughty DV, Vibbert C, Kewalramani A, Bollinger ME, Dalby RN. 2011. Automated actuation of nasal spray products: Determination and comparison of adult and pediatric settings. Automated actuation of nasal spray products. Drug Dev Ind Pharm 37(3):359–366.
14. U.S. Food and Drug Administration 2003. Guidance for industry: Bioavailability and bioequivalence studies for nasal aerosols and nasal sprays for local action.
15. Liu X, Doub WH, Guo C. 2010. Evaluation of droplet velocity and size from nasal spray devices using phase Doppler anemometry (PDA). Int J Pharm 388:82–87.
16. Williams TJ, Gilles JC, Murphy S. 2009. Velocity profiling of sprays from pharmaceutical nasal spray pumps. Respiratory Drug Delivery Europe 2009, ed., R.N. Dalby, P.R.Byron, J. Peart, J.D. Suman, P.M. Young, Lisbon, Portugal. ISSN 1-933722-30-4
17. Inthavong K, Yang W, Fung MC, Tu JY. 2011. External and near-nozzle spray characteristics of a continuous spray atomized from a nasal spray device. Aerosol Sci Technol 46(2):165–177.
18. Inthavong K, Tian ZF, Tu JY, Yang W, Xue C. 2008. Optimising nasal spray parameters for efficient drug delivery using computational fluid dynamics. Comput Biol Med 38(6):713–726.
19. Inthavong K, Tian ZF, Li HF, Tu JY, Yang W, Xue CL, Li CG. 2006. A numerical study of spray particle deposition in a human nasal cavity. Aerosol Sci Technol 40:1034–1045.
20. Kimbell JS, Segal RA, Asgharian B, Wong BA, Schroeter JD, Southall JP, Dickens CJ, Brace G, Miller FJ. 2007. Characterization of deposition from nasal spray devices using a computational fluid dynamics model of the human nasal passages. J Aerosol Med 20(1):59–74.
21. Coates MS, Fletcher DF, Chan HK, Raper JA. 2004. Effect of design on the performance of a dry powder inhaler using computational fluid dynamics. Part 1: Grid structure and mouthpiece length. J Pharm Sci 93(11):2863–2876.

22. Longest PW, Holbrook LT. 2012. In silico models of aerosol delivery to the respiratory tract—Development and applications. Adv Drug Deliv Rev 64(4):296–311.
23. Frank DO, Kimbell JS, Cannon D, Rhee JS. 2012. Computed intranasal spray penetration: comparisons before and after nasal surgery. Int Forum Allergy Rhinol 27(10)21070-21078. [Epub ahead of print.]
24. Kimbell J, Shroeter JD, Asgharian B, Wong BA, Segal RA, Dickens CJ, Southall JP, Miller FJ. 2004. Optimisation of nasal delivery devices using computational models. Respir Drug Deliv 91(233–238).
25. Kimbell JS, Segal RA, Asgharian B, Wong BA, Schroeter JD, Southall JP, Dickens CJ, Brace G, Miller FJ. 2007. Characterization of deposition from nasal spray devices using a computational fluid dynamics model of the human nasal passages. J Aerosol Med 20(1):59–74.
26. Canny J. 1986. A computational approach to edge detection. IEEE Trans Pattern Anal Mach Intell 8(6):679–698.
27. Lin SP, Reitz RD. 1998. Drop and spray formation from a liquid jet. Annu Rev Fluid Mech 30(1):85–105.
28. Lefebvre AH. 1989. Atomization and sprays. New York: Hemisphere Pub. Corporation. p xi, 421.
29. Wen J, Inthavong K, Tu JY, Wang S. 2008. Numerical simulations for detailed airflow dynamics in a human nasal cavity. Respir Physiol Neurobiol 161:125–135.
30. Snyder JA, Grover RO, Jr. VS, Assanis DN. 2004. Transient spray cone angles in pressure-swirl injector sprays. SAE Technical Paper 2004-01-2939, doi:10.4271/2004-01-2939.
31. Inthavong K, Ge Q, Se CMK, Yang W, Tu JY. 2011. Simulation of sprayed particle deposition in a human nasal cavity including a nasal spray device. J Aerosol Sci 42(2):100–113.
32. Doughty DV, Vibbert C, Kewalramani A, Bollinger ME, Dalby RN. 2011. Automated actuation of nasal spray products: Determination and comparison of adult and pediatric settings. Drug Dev Ind Pharm 37(3):359–366.
33. Senecal PK, Schmidt DP, Nouar I, Rutland CJ, Reitz RD, Corradini ML. 1999. Modeling high-speed viscous liquid sheet atomization. Int J Multiphase Flow 25(6–7):1073–1097.